ADVANCED ELECTRONIC MATERIALS
www.advelectronicmat.de

PEDOT:Tosylate-Polyamine-Based Organic Electrochemical Transistors for High-Performance Bioelectronics

Gonzalo E. Fenoy, Catalina von Bilderling, Wolfgang Knoll, Omar Azzaroni, and Waldemar A. Marmisollé**

The construction of organic electrochemical transistors (OECTs) using poly(3,4-ethylenedioxythiophene):tosylate and polyallylamine hydrochloride composites as conducting channel material is presented. The regulation of the polyelectrolyte-to-conducting polymer proportion allows one to easily tune both electronic and ionic characteristics of the transistors, yielding devices with low threshold voltages while preserving high transconductance, which is an essential requisite for the effective integration of OECTs with biological systems. Also, the incorporation of the polyelectrolyte enhances the transient response of the OECTs during the ON/OFF switching, probably due to improved ion transport. Furthermore, the integration of pH-sensitive amino moieties not only improves the pH response of the transistors but also allows for the non-denaturing electrostatic anchoring of functional enzymes. As a proof-of-concept, acetylcholinesterase is electrostatically immobilized by taking advantage of the NH_2 moieties, and the OECTs-based sensors are able to successfully monitor the neurotransmitter acetylcholine in the range 5–125 µM.

1. Introduction

Organic bioelectronics involves the coupling of organic semiconductors with biological systems, including organs, complex tissues, cells, lipid membranes, proteins, and even small molecules.[1] During the last two decades, the field of organic bioelectronics has experienced immense development, which has been mostly propelled by the design and fabrication of novel materials, the advancement in fabrication technologies and the deeper understanding of the transport properties.[2] The proper connection of the organic semiconductor with biological entities allows for the integration of a variety of functions that range from the control of biological processes with high spatiotemporal resolution to the transduction of biological signals into electronic outputs (i.e., sensoring).[3–5]

Conjugated polymers present tunable electronic conduction due to delocalized pi-molecular orbitals, which has driven their widespread application in different fields.[6] Recently, numerous studies have focused on features related to the simultaneous occurrence of ionic and electronic transports.[7] This efficient mixed conduction comprises the basis of numerous organic electrochemical devices, such as supercapacitors and electrochromic devices.[8–10] Moreover, their soft and biocompatible character make them a very appropriate material for the construction of varied bioelectronic devices, including soft actuators,[11] organic electronic ion pumps,[12] neural probes,[13] and organic electrochemical transistors (OECTs).[14,15]

OECTs, particularly, make use of ion injection from electrolyte solution in order to modulate the conductivity of the organic channel. The coupling between both ionic and electronic charges provides the devices with high transconductance compared with that of field effect transistors, but also limits their response time.[14,16] While poly(3,4-ethylenedioxythiophene) (PEDOT):PSS is the quintessential material for the fabrication of OECTs, one of its main drawbacks involves the operation in depletion mode, which means that the channel is initially in the conducting state and the application of a gate voltage is required to switch off the device.[17] This intrinsic doping produces high operating currents and demands the use of high gate voltages (≈0.8 V vs Ag/AgCl) to maintain the channel in

G. E. Fenoy, Prof. C. von Bilderling, Prof. O. Azzaroni, Prof. W. A. Marmisollé
Instituto de Investigaciones Fisicoquímicas Teóricas y Aplicadas (INIFTA)
Departamento de Química, Facultad de Ciencias Exactas
Universidad Nacional de La Plata (UNLP) – CONICET
64 and 113, Buenos Aires 1900, Argentina
E-mail: azzaroni@inifta.unlp.edu.ar; wmarmi@inifta.unlp.edu.ar

The ORCID identification number(s) for the author(s) of this article can be found under https://doi.org/10.1002/aelm.202100059.

DOI: 10.1002/aelm.202100059

G. E. Fenoy
Instituto de Investigación e Ingeniería Ambiental
Universidad Nacional de San Martín
25 de Mayo y Francia, 1 piso, Buenos Aires 1650, Argentina
Prof. W. Knoll
CEST – Competence Center for Electrochemical Surface Technologies
Konrad Lorenz Strasse 24, Tulln 3430, Austria
Prof. W. Knoll
Austrian Institute of Technology (AIT)
Donau-City-Strasse 1, Vienna 1220, Austria
Prof. O. Azzaroni
CEST-UNLP Partner Lab for Bioelectronics (INIFTA)
Diagonal 64 y 113, La Plata 1900, Argentina

the OFF condition. Then, when operating in solution, this relatively high gate voltage (V_G) can trigger parasitic reactions with water and oxygen, prompting device deterioration.[18,19] Hence, the development of channel materials which endow the use of low gate voltages, and, consequently, reduce power consumption and avoid parasitic reactions, is of crucial interest.

Moreover, when considering the connection with biological entities, PEDOT:PSS presents some drawbacks related to the low (bio)functionality of PEDOT and the acidity/toxicity of PSS.[20] In addition, the overall anionic charge of the conducting polymer–polyelectrolyte complex limits its interaction and integration with negatively charged entities, such as cells, DNA/RNA, and most proteins at physiological pH conditions.[21,22] This aspect becomes particularly relevant when considering the construction of biosensors, whose performance critically depends on the properties of the interfacial bio-architecture. In this sense, enzymes must be immobilized in a way that preserves and guarantees their biological activity, ensuring accessibility to the active sites and avoiding the hampering of the transduction mechanism.[23,24]

Regarding these two aspects, the incorporation of amine moieties in the channel material of OECTs has been recently reported as an effective approach to conveniently tune the features of the transistors, such as ionic transport properties and pH sensitivity. For instance, the operation voltage range of OECTs have been previously modulated by dedoping with polyethyleneimine (PEI) and also with vapors of commercially available aliphatic amines.[19,25] In the same sense, Cea et al. have developed a composite of PEDOT:PSS and PEI to fabricate OECTs exhibiting stable operation and high transconductance.[26] Furthermore, Zeglio et al. have demonstrated that hydrophobic PEDOT-S:ammonium salt complexes are excellent candidates for the production of high-performance water-based OECTs.[27]

The incorporation of amines was also demonstrated to allow for further functionalization of the PEDOT surface in order to create efficient bioelectronic interfaces. Very recently, Mecerreyes and coworkers have reported the chemical oxidative (co)polymerization of 3,4-ethylenedioxythiophene (EDOT) and EDOT-ammonium derivatives leading to PEDOT-N (co) polymers, which show biocompatibility in the presence of the human embryonic kidney-293 cell line.[20] Furthermore, the integration of polyamines in the PEDOT matrix has been proved to be an effective strategy for conferring anchoring sites for further biofunctionalization without drastically disrupting the electronic properties of the conducting polymer.[28,29]

Finally, regarding OECT-based biosensors fabrication, the immobilization of enzymes on amine-functionalized surfaces has been shown as an effective approach to fabricate graphene and organic transistors-based biosensors.[24,30] For instance, Buth et al. modified the surface of α6T-based OECTs with APTES and found that the acid–base equilibrium of surface amino groups was able to change the doping state of the channel material, causing a shift in the threshold voltage and, by thus, increasing the pH sensitivity of the devices.[31] In this regard, the integration of cationic polyelectrolytes has also increased the pH sensitivity and enzyme anchoring capability in graphene-based FET biosensors.[24]

Herein, we report a simple method to build OECTs using polyallylamine hydrochloride (PAH) as co-dopant of chemically synthesized PEDOT in the presence of iron (III) *p*-toluenesulfonate (tosylate, TOS) as dopant. The adjustment of the polyelectrolyte-to-conducting polymer proportion allows us to easily tune both electronic and ionic features of the transistors, yielding devices with low threshold voltages while maintaining high transconductance. Likewise, the incorporation of PAH enhances the transient response of the OECTs, probably due to an improved ion transport through the film. Furthermore, the integration of PAH also improves the pH response of the transistor and allows for the electrostatic anchoring of acetylcholinesterase (AchE) by taking advantage of the NH_2 moieties. Later, the AchE-functionalized OECTs can perform the successful sensing of the neurotransmitter acetylcholine. As far as we know, this is the first report for the fabrication of polyamine-PEDOT:TOS OECTs, exploiting the excellent electronic properties of the chemically obtained PEDOT:TOS films while enabling the manipulation (and enhancement) of key OECTs features by the integration of the polyamine.

2. Results and Discussion

2.1. Fabrication and Performance of the Organic Electrochemical Transistors

OECTs were prepared by in situ chemical polymerization of the channel material on commercial interdigitated electrodes (IDEs) by spin coating (**Figure 1**A). PEDOT and PEDOT–PAH OECTs were prepared, and different polyelectrolyte to conducting polymer ratios in PEDOT–PAH films were investigated. The different PAH to PEDOT ratio yielded PEDOT–PAH1, 2, and 3 OECTs (see Supporting Information and Experimental Section).

In order to perform the OECTs measurements, an electrolyte gated configuration was used, as shown in Figure 1A. We found that a few dedope/redope cycles were required in order to acquire a stable time response for the transistors, attributed tentatively to the hydration of the polymer film during the first cycles, as recently reported.[32] The output characteristic curves of a PEDOT and a PEDOT–PAH3 transistors are shown in Figures 1B and 1C, respectively (Figure S1, Supporting Information, shows the curves for PEDOT–PAH1 and PEDOT–PAH2). It can be seen that the devices work in depletion mode, that is, in the absence of a gate voltage, the devices display the ON state.

The spin-coating technique allowed for a reproducible and homogeneous film deposition, as shown by the atomic force microscopy (AFM) images of the channel section for different transistors (**Figure 2** and Figure S2, Supporting Information). The thicknesses of the polymer channel of the devices were also obtained by AFM measurements and are shown in Figure S3, Supporting Information. Furthermore, the use of IDEs combined with the highly conductive polymer PEDOT:TOS resulted in very high device transconductance values while allowing for a stable response, as well as high device-to-device reproducibility (the RSD of conductivity values for the finished OECTs was lower than 5% for 15 transistors). Additionally, the

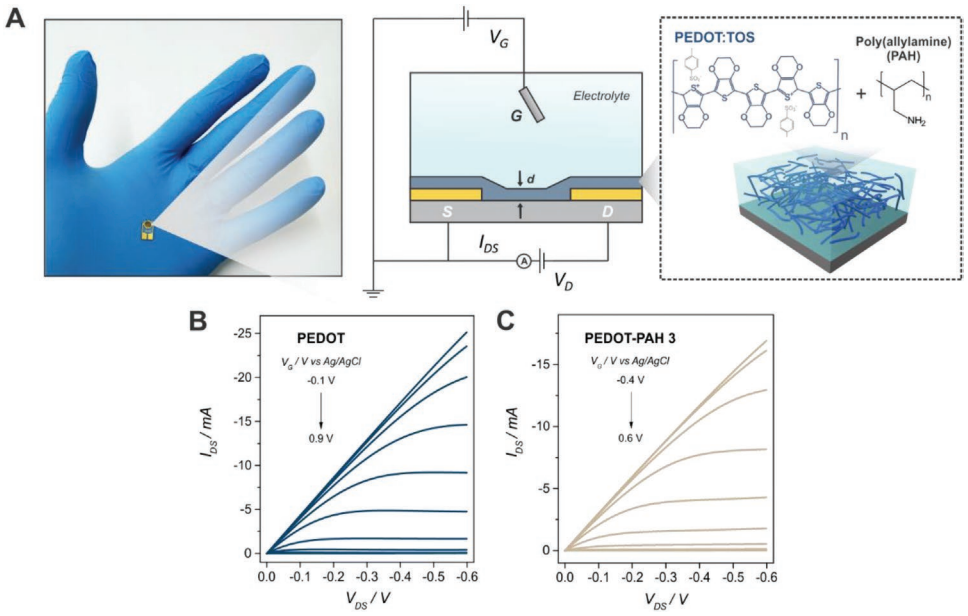

Figure 1. A) Scheme showing an OECT, the measurement setup used and a representation of the polyelectrolyte-conducting polymer blend. B) Output curves for a PEDOT and C) PEDOT–PAH3 OECT (0.1 M KCl pH 7).

changes in resistance after a complete set of experiments were monitored, showing variations lower than 3% for all the studied transistors, which accounts for the high stability of the devices (Figure S4, Supporting Information).

The transfer characteristics for the different OECTs are shown in Figure 2A. A shift in the threshold voltage (V_{th}) is obtained when adding PAH to the polymerization solution (PEDOT–PAH1, 2, and 3 OECTs): the threshold voltage shifts to more negative values when increasing the PAH to PEDOT ratio. To quantify these changes, we extracted the V_{th} from the transfer curve plotted in the linear scale (Figure S5, Supporting Information). The importance of extracting the V_{th} from the linear regime roots in the uniformity of the charge distribution along the channel observed under these conditions.[33]

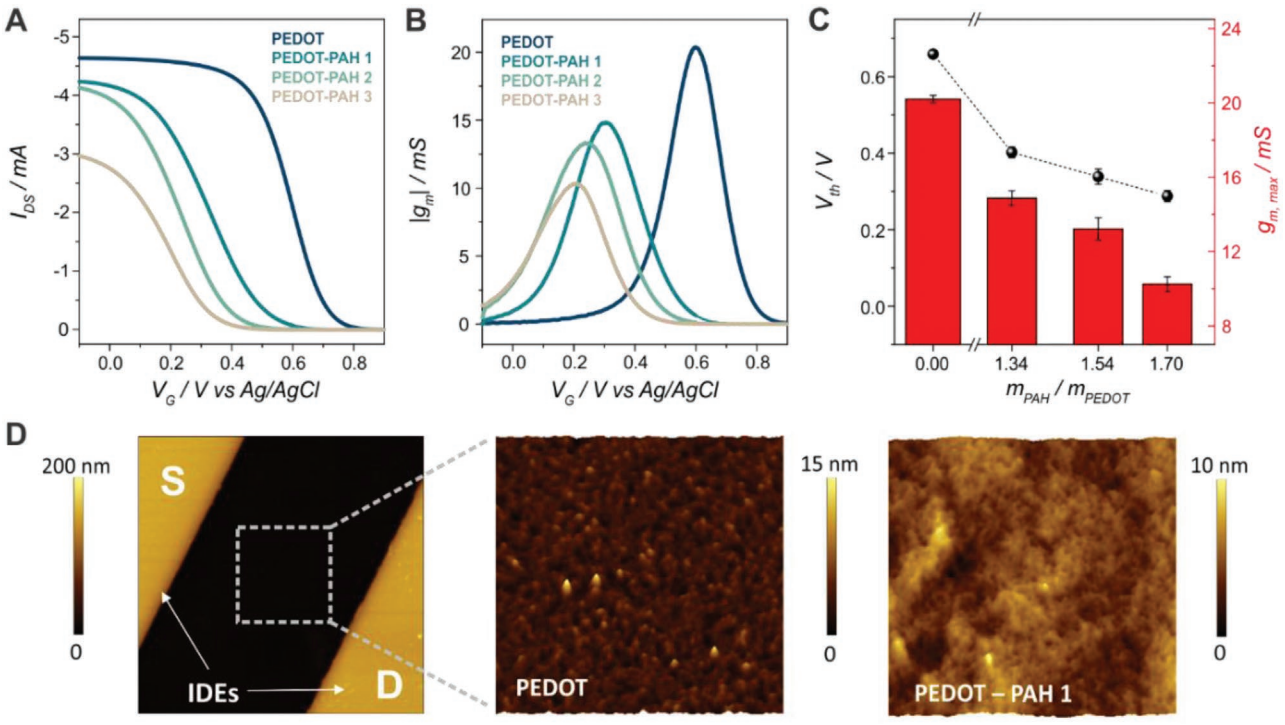

Figure 2. A) Transfer characteristics, B) transconductance, and C) threshold voltages and maximum transconductances obtained values for the different OECTs (KCl 0.1 M pH 7, V_{DS} = –0.1 V). D) AFM topography images of a PEDOT (left) and a PEDOT–PAH1 (right) transistor.

By adding PAH to the polymerization solution, the threshold potential values of the transistors are shifted by −0.26, −0.32, and −0.37 V with respect to the pristine PEDOT values (PEDOT–PAH1, 2, and 3, respectively, Figure 2A,C). In this sense, the shift obtained for PEDOT–PAH3 transistors is among the highest reported for OECTs using polymer blends as channel materials. For instance, Schmode et al. have recently reported the copolymerization of ion-conducting together with hole-conducting 3-hexylthiophene monomers, and found the highest shift in the threshold voltage to be 0.25 V.[34] Recently, different amines addition to PEDOT:PSS transistors caused shifts up to −0.35 V.[19] Finally, Zeglio et al. reported ammonium-salt self-doped PEDOT transistors, which showed a shift in the threshold potential of 0.2 V when compared with PEDOT-S transistors.[27]

Moreover, state-of-the-art devices using commercial PEDOT:PSS as channel material have reported a V_{th} of ≈0.52 V.[35] Then, while PEDOT OECTs showed higher V_{th} values, it is observed that the incorporation of PAH on the channel material generates lower threshold voltages. This result accounts for better integration of both insulating and conducting phases in PEDOT:PAH OECTs compared to a widely employed commercial material by making use of a straightforward synthetic approach.

The shift in the threshold voltage has been attributed to different effects. One of them involves the improvement of the overall ion mobility of the polymer blend used as the channel material of the transistors. In this way, the incorporation of the polyelectrolyte into the conducting matrix involves the formation of hydrophilic domains that facilitates ion percolation mechanisms and, thus, reduces the voltage required to switch off the devices. The improvement of the ion mobility has been extensively studied in films and OECTs obtained from the commercial formulation of PEDOT:PSS, PEDOT:TOS–gelatin composites, and other OECTs.[32,34,36] Some authors have even reported an enhancement of the percolation pathway while adding a cationic polyelectrolyte to PEDOT:PSS films.[37] Moreover, as the ion-conducting phase in the films does not play a direct role in the charge-compensation of PEDOT (in contrast with PEDOT:PSS), anion movement becomes more important in the doping–dedoping process, being facilitated as NH_2 moieties from the polycation are incorporated.[36] Another well-documented mechanism for threshold voltage shifting involves the dedoping caused by amines. Different authors have reported the incorporation of aliphatic amines in PEDOT:PSS OECTs in order to dedope the channel material and diminish the threshold voltage of OECTs.[19,38] However, in our case, we do not observe a considerable conductivity diminution in the OECTs upon PAH addition in the channel material (Figure S4, Supporting Information).

In this sense, when incorporating an insulating phase to the channel material, one would expect the electronic conductivity to be greatly hindered, particularly when considering high ratios as the ones used in this work. Interestingly, the incorporation of PAH yields no significant detriment in the drain–source current in the case of PEDOT–PAH1 (it is only diminished by 8.4%) and PEDOT–PAH2 (10.6% decrease) OECTs. Some hindering of the electronic transport through the channel is evidenced only for the case of the highest PAH proportion, as a considerable reduction of the ON I_{DS} of 35.9% is found, even when the polymer channel thickness was markedly increased. Results obtained from the measurements of the resistance of the as-prepared composite film in air at ambient temperature support these findings, as the film resistance between the source and drain electrodes was found to increase with the PAH ratio in a similar fashion to the decrease found in I_{DS} (Figure S6, Supporting Information). Similar findings have been reported for PEDOT:TOS–gelatin composites, where insulating:conducting polymer ratios higher than 2:1 showed a steep decrease in the conductivity of the composites.[36]

Another key figure of merit of OECTs is the transconductance, which is involved in every mechanism and application concerning transistors, and particularly in biosensing, as a high transconductance is a requirement for the development of highly sensitive devices.[24,39] From Figure 2B,C, it can be noticed that the obtained transconductance values follow the same tendency as that observed for the ON I_{DS} values. It is observed that, upon PAH addition, transconductance values decreases by 26% (PEDOT–PAH1), 34% (PEDOT–PAH2), and 49% (PEDOT–PAH3). The obtained transconductances are still among the highest reported for OECTs, particularly when considering the low drain–source voltage employed, which makes this approach an efficient and straightforward strategy for the construction of high-performance transistors.[40]

Thus, the incorporation of PAH into the PEDOT:TOS matrix can be employed to modulate the threshold potential while maintaining high values of transconductance in the OECTs. As it will be shown later, the addition of PAH also enhances the transient features, pH-responsiveness, and allows for the anchoring of functional enzymes for the construction of biosensors.

2.2. Ultraviolet–Visible Spectroelectrochemistry

With the aim of gaining more insight into the electrochemical and optical features of the composite films, we performed spectroelectrochemistry measurements. The same deposition procedure previously described was followed using indium tin oxide (ITO) plates as substrates, which constituted the working electrode in the experimental setup described in the **Figure 3**A.

The spectra of a PEDOT–PAH2 composite-modified ITO substrate at different applied potentials (vs Ag/AgCl reference electrode) are shown in Figure 3B. The spectrum of the as-synthesized film was included for comparison. As expected, the features of the spectrum showed no major changes upon the addition of PAH with respect to a typical PEDOT:TOS spectrum.[41] It can be seen that, in the fully reduced state, the spectrum shows a band at ≈630 nm, ascribed to π–π^* transitions, which is responsible for the deep blue color of the reduced films. When more positive potential values are applied, the polymer is switched to its conducting state and a wide band in the near IR emerges, ascribed to the absorption of the polaronic and bipolaronic units in the polymer. Simultaneously, the π–π^* band steeply vanishes and the polymer develops a sky-blue color.[8,41]

The formal redox potential ($E^{o'}$) of the composite film can be obtained by plotting the change in absorbance at a relevant wavelength (for example that of the π–π^* transition) as

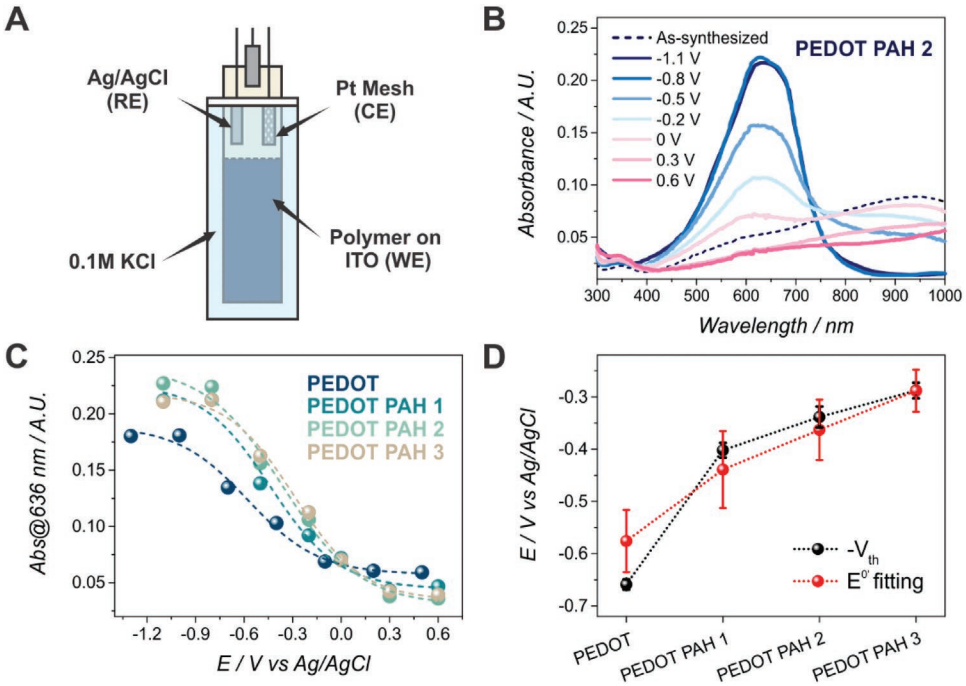

Figure 3. A) Scheme of the setup used in the spectroelectrochemistry measurements. B) Spectra at different potentials of a PEDOT–PAH2-coated ITO substrate, together with the spectrum of the as-synthesized material. C) Absorbance at 636 nm at different potentials for the different polymer-coated ITO substrates together with the fitting to a sigmoidal curve. D) Comparison of the V_{th} values extracted from the transfer characteristics with the $E^{o'}$ values obtained from the fitting.

a function of the applied potential. As the redox transition in PEDOT is related to the change in the conductivity regimes, the formal redox potentials are expected to be related to the threshold voltage values obtained when employing the transistor configuration (while some variances could appear due to the difference in the setups and substrates used[42]). The changes in the absorbance at 636 nm as a function of the applied potential were plotted for the different composite films and fitted to a sigmoidal dependence to obtain the $E^{o'}$ values (Figure 3C). The obtained $E^{o'}$ value for PEDOT matches with previous reported values, supporting the spectroelectrochemical method.[41] Moreover, the obtained $E^{o'}$ values shift to more positive/less negative potentials as the PAH-to-PEDOT ratio in the films increases (Figure 3D). Thus, the introduction of PAH in the polymer films stabilizes the reduced form of PEDOT in comparison with the oxidized form, shifting the formal redox potential to higher values. This trend is similar to that found for V_{th} in the transistor configuration. We should note here that the differences in notation coming from two different fields result in a discrepancy in the sign of both values, but the physical meaning remains related. The $E^{o'}$ values obtained from the sigmoidal fitting of the spectroelectrochemical results and the V_{th} obtained from the transfer characteristics are comparatively presented in Figure 3D. The good correlation between $E^{o'}$ and $-V_{th}$ values supports the hypothesis of a facilitated reduction process in PAH-doped films, causing the shifting of the threshold potential. Finally, spectroelectrochemistry measurements constitute a valuable approach to study the changes in the redox potential upon varying the composite composition, disentangling coupled effects observed in the performance of the OECTs.

2.3. Transient Behavior

Another important feature of OECTs is the transient behavior, particularly when considering their application in biological environments.[43] In order to study the kinetics involved in device switching, the transient responses for OECTs fabricated with each PAH to PEDOT ratio have been investigated. As depicted in **Figure 4**A,B, the repeated cycling of the OECTs between the ON and OFF states was performed using a square-wave applied gate potential while recording the drain–source current at a constant drain voltage. According to previous works,[43,44] the source–drain current response was adjusted to an exponential decay in order to obtain t_{on} and t_{off} for each set of transistors. Curves obtained for PEDOT and PEDOT–PAH2 are comparatively shown in Figure 4, whereas measurements for the other composites are shown in the Figure S7, Supporting Information.

From Figure 4C, it can be noticed that for PEDOT–PAH1 and 2 OECTs the addition of the polyamine to the PEDOT matrix reduces the ON and OFF times, which can be explained by a more effective ion transport caused by the added polyelectrolyte. It has been reported that the time response of an OECT to a square voltage pulse on the gate is related to the charging of an "'effective"' capacitor, and consequently it is affected by the ion percolation ability of the polymer channel. Then, the shorter switching times for the blends PEDOT–PAH1 and 2 with respect to PEDOT could be ascribed to an enhanced ion transport as a result of the PAH incorporation. In the case of PEDOT–PAH3 OECTs, it can be observed that the response is hindered, probably

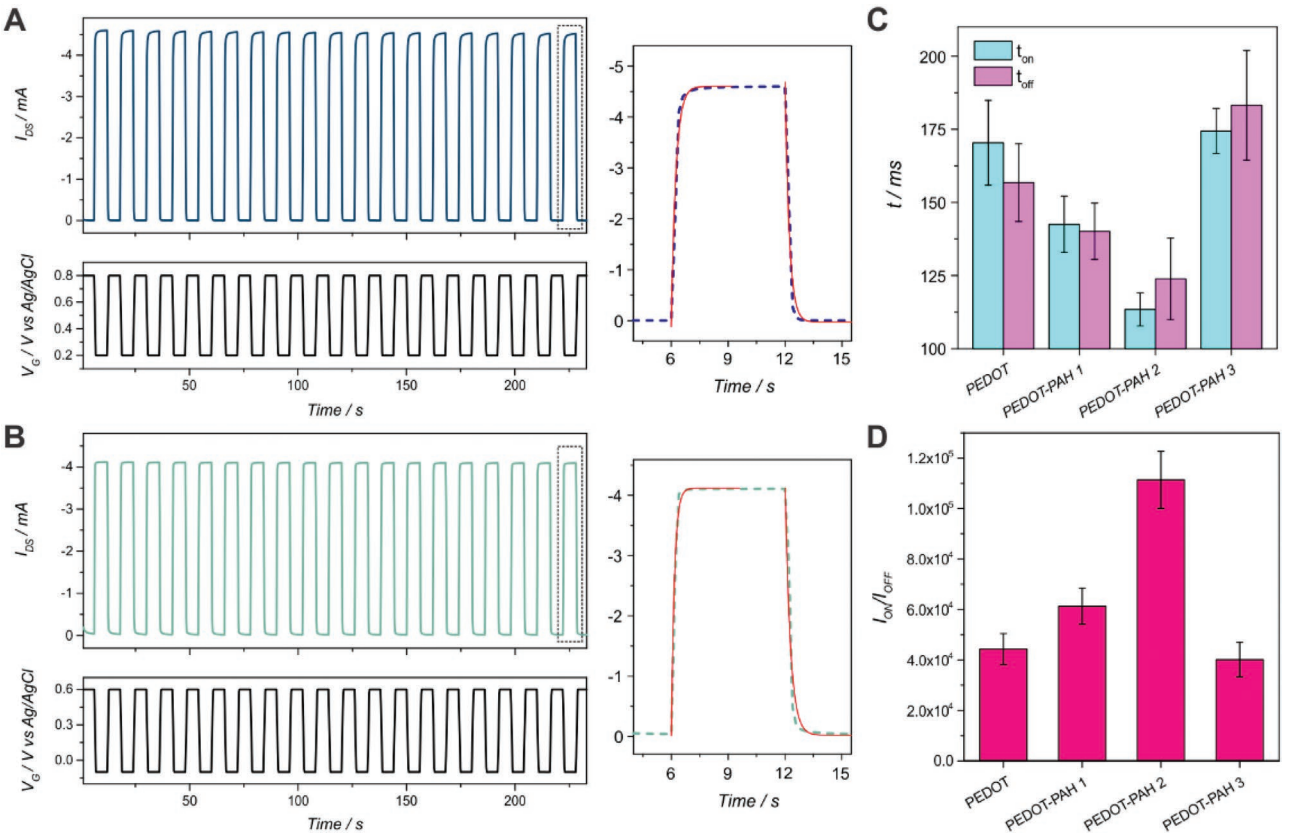

Figure 4. Transient characteristics and example of the exponential fitting for A) PEDOT and B) PEDOT–PAH2 OECTs (V_D = –0.1 V, 0.1 M KCl pH 7). C) Switching ON and OFF times values obtained from the fitting of the transient characteristics. D) I_{ON}/I_{OFF} ratios obtained for the different transistors.

by a decrease in the electronic transport efficiency. In line with these findings, the increase on the response time when high ratios of a less conducting material was incorporated on the channel material was also reported for other conducting polymer blends, as 2:1 or 3:2 PTEB-S:PEDOT-S blends OECTs.[45]

Another relevant parameter of OECTs is the I_{ON}/I_{OFF} ratio, which is especially important in applications such as logic circuits and matrix active displays.[46] The I_{ON}/I_{OFF} ratios obtained from the transfer characteristics curves for each composition are shown in Figure 4D. The parameter follows a dependence on PAH proportion similar to that observed for the dynamic behavior. This phenomenon could also be ascribed to the improved ion percolation through the films in which PAH was incorporated, which facilitates the complete reduction of the channel material. It is known that the I_{ON}/I_{OFF} ratio is not only dependent on the conductivity of the channel, but also on its capacitance and doping level.[46] Moreover, the reduced redox state (OFF condition) can be electrostatically stabilized by interaction with charged PAH residues (as observed on the redox potential trend of the composite), facilitating the channel switching off and resulting in a lower OFF current. In this way, the dedoping effect by different amines on PEDOT-based transistors has been extensively studied in the recent years.[38] Later, higher ratios of PAH resulted in a lower OFF-state current but simultaneously reduced the ON state current, showing the best interplay for PEDOT–PAH2 OECTs. A similar trend for the dependence of the ON/OFF ratio on the polyamine proportion was observed for PEDOT:PSS-PEI transistors.[26]

Recently, a decrease of stability upon ON/OFF switching was reported for transistors made of conjugated polyelectrolytes blends as channel materials.[45] However, in our case, all of the transistors studied showed excellent stability as a current decrease of less than 1% was found to occur after more than 20 ON/OFF cycles.

Thus, it can be stated that PAH incorporation causes no additional barrier for ion migration both in and out of the film during the dedoping/doping process. On the contrary, it even improves the ionic transport through the channel material and consequently the transient response and the I_{ON}/I_{OFF} ratio of the devices.

2.4. Electrochemical Impedance Spectroscopy Characterization

In order to gain more insight into the electronic and ionic processes taking place in the OECTs, potentiostatic EIS measurements were performed for the different polymer channel materials. It has been previously stated that the OECT behavior can be taken as a combination of an electronic circuit, which accounts for charge transport in and to the channel material, and an ionic circuit, which is related to the ionic transport from the electrolyte to the polymer.[44,47] While several circuits have been developed for conducting polymer electrodes, and particularly

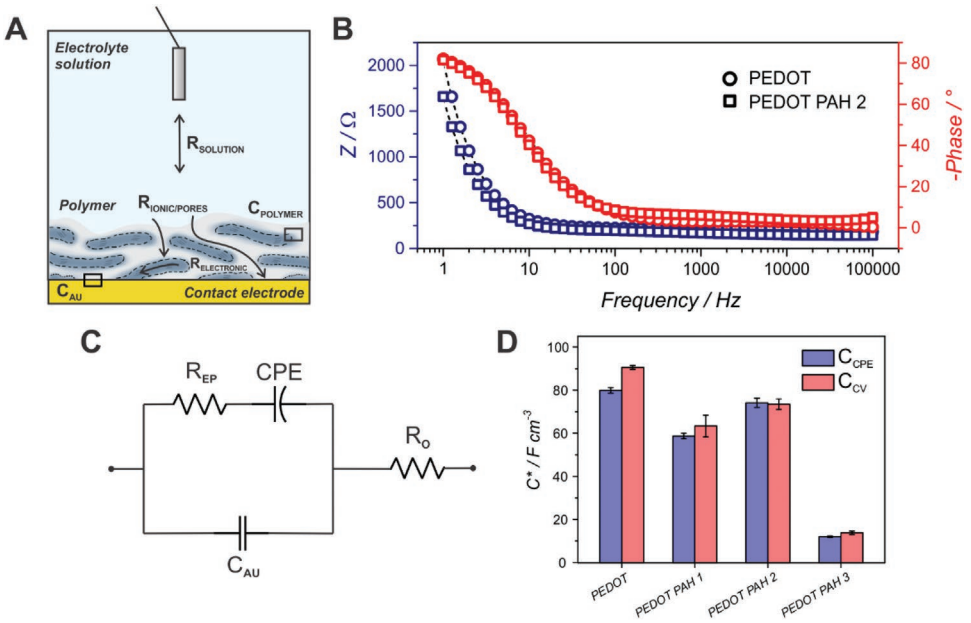

Figure 5. A) Scheme of the different processes taking place in the films. B) Bode plot for the impedance spectrum of a PEDOT and a PEDOT–PAH2 electrode. C) Equivalent circuit used for fitting the impedance data and D) volumetric capacitance for the different films obtained from CV and EIS measurements.

for PEDOT:PSS, the interpretation of the EIS response of conducting polymers is not simple.[48] **Figure 5**A shows a schematic picture of the charge transport processes that take place, whereas a more detailed description of the EIS model can be found in Supporting Information.

We keep the minimum complexity of the equivalent circuit to account for the changes in the experimental EIS response (Figure 5B). Briefly, the circuit employed to fit the EIS results (Figure 5C) includes the base metallic electrode–inner solution interface capacitance (C_{Au}), which is connected in parallel to a series connection of the R_{EP} resistance, containing contributions from the electronic resistance of the polymer domains and the resistances ascribed to ionic transport needed for charge compensation, and a constant phase element (CPE), which accounts for the polymer domains–inner solution interface capacitance.[49–52] Typically, when the electrode surface is rough, the charging/discharging features of the interface cannot be precisely described with a capacitive element, and a CPE is employed.[48] The impedance of the CPE is described by $Z_{CPE} = Yo^{-1}(j\omega)^{-n}$, and the magnitude of the deviation from the capacitive behavior is defined by n. When $0.8 < n < 1$, the CPE can be considered as a capacitance. Finally, a resistance is connected in series, which is ascribed to a sum of the ionic transport resistance through the film porosity and the electrolyte solution resistance.[51,53]

The Bode plots for PEDOT and PEDOT–PAH2 polymer film electrodes at 0V are shown in Figure 5B together with the predicted values from the fitted parameters (Bode plots for the other OECTs are shown in the Supporting Information). The fitting reveals that the experimental EIS data can be satisfactorily described by the proposed simplified model for all the OECTs and fitted parameters for all the OECTs are shown in **Table 1**.

Then, R_O comprises the high frequency resistance and it is ascribed to a series combination of the solution resistance and the resistance ascribed to the ionic transport through the porous (whether is only PEDOT or PEDOT–PAH) structure of the polymer film.[51] As the solution resistance should be constant when employing the same electrolyte solution, the difference in the values obtained from the fitting can be ascribed to a difference in the ionic transport resistance through the channel material. Then, from Table 1, it is observed that R_O shows a value of 188.7 Ω for PEDOT, while it decreases by 25% for PEDOT–PAH1, by 23% for PEDOT–PAH2, and by 34% for PEDOT–PAH3. The addition of PAH decreases the ionic resistance through the porous structure of the channel material,

Table 1. Equivalent circuit parameters obtained by fitting the EIS data for each composite material film electrode.

	C_{Au} [μF]	R_{EP} [Ω]	R_O [Ω]	Y_0 [S.s^n]	n_{CPE}	C_{CPE} [μF]
PEDOT	1.76	30.9	188.7	8.30E − 05	0.96	79.9
PEDOT–PAH1	3.83	39.2	141.1	9.10E − 05	0.95	58.7
PEDOT–PAH2	3.45	48.0	145.4	1.01E − 04	0.96	74.1
PEDOT–PAH3	2.86	51.2	124.9	5.00E − 05	0.93	12.0

Table 2. Relevant features obtained for the different OECTs.

	Thickness [nm]	m_{PAH}/m_{PEDOT}	$g_{m\ max.}$[mS]	V_{th} [V]	I_{on}/I_{off}	t_{on} [ms]
PEDOT	75	0	20.2	0.66	4.43E + 04	170.4
PEDOT–PAH1	114	1.34	14.9	0.40	6.13E + 04	142.5
PEDOT–PAH2	106	1.54	13.2	0.34	1.11E + 05	113.4
PEDOT–PAH3	248	1.7	10.3	0.29	4.02E + 04	174.4

enabling an improved ionic transport. In this sense, the PEDOT film can be imagined as a more compact film exhibiting only one type of material which is conducting and whose porous structure could be ascribed to the own porosity of the conducting polymer when synthesized. However, when considering PEDOT–PAH blends, the polymer composites show a mixed structure, which allows for a more efficient ionic transport coming from both porous structure and enhanced ionic transport due to polyelectrolyte incorporation.

On the other hand, C_{Au} is ascribed to the Au contact electrode–inner solution electrolyte interface capacitance. As expected, this capacitance is lower compared to that of the conducting polymer–electrolyte interface (depicted as a CPE element) (Table 1). It can be observed that the values obtained for the capacitive element are higher for all the blends containing PAH compared to that of PEDOT. This outcome can be explained as the film containing only PEDOT is more compact and homogeneous when compared with the PAH-containing blends, exhibiting a lower fraction of base electrode–internal media interface compared to PEDOT–PAH1, 2, and 3.

The so-called R_{EP} resistance has contributions from both the overall ionic resistance through the porous film (whether it is linked to the charge transfer process in PEDOT or not) and the polymer electronic charge transfer resistance. From Table 1, it can be observed that values obtained for this resistance are higher in every PAH-containing blend when compared to PEDOT, showing a steady increase with PAH concentration. This result accounts for the decrease of the electronic component of the charge transport processes across the OECT channel as the proportion of the electrochemically inactive component is increased.

Finally, the CPE element is considered. As the obtained n values were higher than 0.9 for all the OECTs channel materials (Table 1), the CPE element is interpreted as a capacitance, and the corrected capacitance values for the CPE are reported. Therefore, for an adequate comparison, the values were normalized by the measured film volume to determine the volumetric capacitance (C^*). It can be observed that PEDOT transistors show higher volumetric capacitance compared with all the other composite materials in which PAH was added to the polymerization solution. This is consistent with the lower proportion of electroactive material within the polymer films. When considering the three blends of the conducting polymer with PAH, PEDOT–PAH2 shows the highest volumetric capacitance. Furthermore, it can be observed that PEDOT–PAH3 transistors show the lowest volumetric capacitance values, which can be ascribed to the higher amount of non-conducting material incorporated.

These capacitances obtained from the EIS analysis were further compared with the voltammetric capacitances computed from CV measurements in a potential region where no reaction is known to occur (see Figure S10, Supporting Information). Figure 4D shows the comparison between the volumetric capacitances obtained from both EIS and CV measurements. The excellent agreement confirms the values of volumetric capacitance obtained from EIS data and validates the equivalent circuit proposed on Figure 5C.

Usually, the incorporation of bulky ionic or polyelectrolytic dopants to the electroactive component of the OECT channel yields low values of the volumetric capacitance ($C^* < 50$ F cm^{-3}). Although the incorporation of these ionic components produces more efficient swelling and faster ion transport, the "dead volume" arising from the overabundant insulating phase lowers the C^* values. This is the case for the composite PEDOT:PSS, the most employed OECT material, which shows a C^* of 39 F cm^{-3}.[17] In the case of PEDOT–PAH1 and PEDOT–PAH2, however, the addition of PAH does not dramatically reduce the volumetric capacitance values. This relatively high capacitance values ($C^* > 50$ F cm^{-3}), combined with the improved ionic transport with respect to PEDOT, result in OECTs displaying very interesting transfer and transient performances. Both ionic resistance and volumetric capacitance can be regarded as components of a more general phenomenon regarding the ionic transport ability of the PAH-doped transistors. Within this framework, EIS becomes a powerful tool to investigate the underlying processes and reach a better understanding of the behavior of the OECTs.

Table 2 resumes the most important features of the transistors for the different PAH to PEDOT ratios. In this regard, when considering the transient features, the high ionic/pore resistance contributes to the slower transient response in PEDOT OECTs. On the other hand, a high PAH to PEDOT ratio, as in the case of PEDOT–PAH3 transistors, diminishes the resistance to the ionic transport, but the low proportion of the electroactive component dramatically affects the volumetric capacitance and the transconductance of the devices. On the contrary, in the case of PEDOT–PAH1 and PEDOT–PAH2, the trade-off between the electronic resistance and the ionic conductance yields the best transient features in terms of the ON/OFF times, retaining satisfactory values of I_{DS} and transconductance.

2.5. pH Response Improvement

In the last years, the use of OECTs for sensing applications has shown enormous progress, achieving the successful detection of a variety of biologically relevant analytes.[39,54–56] However, it has been stated that the pH sensitivity of PEDOT:TOS is rather low,[57,58] which hampers its use in pH-based sensing

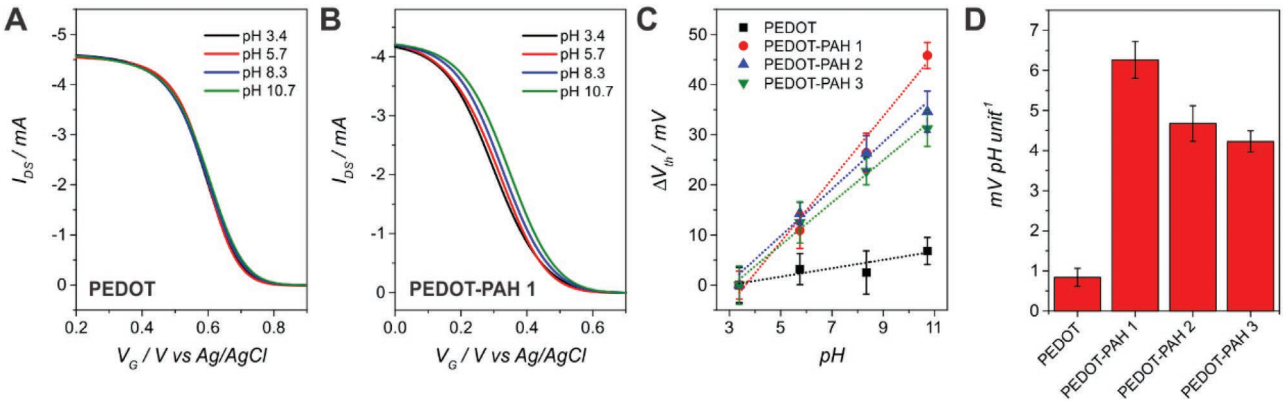

Figure 6. Transfer characteristics for A) a PEDOT and B) a PEDOT–PAH1 OECT while increasing the pH of the electrolyte (V_{DS} = −0.1 V, 0.1 M KCl). C) Change in V_{th} with the pH of the solution and linear fitting for the different OECTs. D) Sensitivity obtained from the linear fitting for the different transistors.

devices. The same has been observed for PEDOT:PSS, as the sulfonate moieties function as the counterion in the complex and, moreover, they show a pK_a around 2.[59] In order to overcome this problem, the incorporation of pH-sensitive moieties to the channel material has been reported as an effective approach.[24,31,60,61]

Then, we studied the pH sensitivity of the transistors fabricated with different PAH to PEDOT ratios. **Figure 6** shows the transfer characteristics of the different OECTs while changing the pH of the electrolyte solution at constant ionic strength (0.1 M KCl) (for the sake of clarity, only results for PEDOT (Figure 6A) and PEDOT–PAH1 (Figure 6B) OECTs are shown, while Figure S11, Supporting Information, shows the results for PEDOT–PAH2 and PEDOT–PAH3 OECTs). For PEDOT–PAH transistors, it can be observed that a decrease in the pH of the electrolyte solution shifts the threshold voltage of the devices toward more negative values. On the other hand, PEDOT transistors show almost no shifting, in agreement with previously reported results.[58]

The effect observed in PAH-modified transistors can be explained in the following way: as the pH decreases, a higher proportion of amine moieties in the composite become charged and, therefore, are able to dedope/change the doping state in the PEDOT conducting phase by electrostatic screening of the TOS counterions, which shifts the threshold voltage to more negative values. In this way, Johansson et al. have reported a similar behavior concerning the doping in PEDOT-S:alkyl ammonium salts complexes with the pH.[62] Moreover, the shift in the threshold voltage of amine-functionalized α6T OECTs with the pH was reported by Buth et al.,[31] and a similar effect was observed in graphene field-effect transistors functionalized with different amino moieties.[24,63]

Figure 6C shows that PEDOT–PAH1 OECTs exhibit the highest pH sensitivity, that, 6.3 ± 0.5 mV/pH unit, while PEDOT–PAH2 devices show a value of 4.7 ± 0.4 mV/pH unit (three different measurements performed). Finally, PEDOT PAH 3 transistors show a pH sensitivity of 4.2 ± 0.3 mV/pH unit. The highest pH sensitivity of the PEDOT–PAH1 OECTs could be related to the more homogeneous film formed for this PAH to PEDOT ratio, as shown from AFM roughness measurements, which would allow a more intimate connection between the NH_2 moieties-bearing polyelectrolyte regions and the PEDOT conducting phase (AFM measurements in Supporting Information). In this way, the increase in roughness for PEDOT–PAH2 and PEDOT–PAH3 OECTs goes in line with this hypothesis, as these transistors showed increased roughness and decreased pH sensitivity.

Furthermore, the devices displaying the highest pH sensitivity (PEDOT–PAH1 OECTs) were also tested in a flow configuration, where different pH solutions were flowed using a PMMA flow cell (Figure S13, Supporting Information). We have also performed CV experiments employing $Ru(NH_3)_6^{+2/+3}$ couple as molecular probe in order to study the pKa of the PEDOT–PAH1 composites, obtaining a value of 7.9 ± 0.3 (Figure S12, Supporting Information).

One of the advantages of our approach for the derivatization of the polymer channel is that the PAH incorporation produced just a slight diminution in the transconductance, while in some recent works the modification of the channel in order to improve the pH sensitivity was found to seriously deteriorate the performance of the transistors.[31] Then, although the present pH sensitivities are lower than those reported for other transistors,[24,31,60,64] the changes in V_{th} with pH are sufficient to account for an easily observable change in I_{DS} in the flow setup due to the high transconductances of the devices.

2.6. Biosensors Fabrication

The incorporated amino moieties could also serve as anchoring sites for the subsequent immobilization of enzymes for the construction of biosensors. In this way, the use of PEDOT–PAH composites films has been shown successful when dealing with the immobilization of GOx and other enzymes onto PET and plexiglass-modified substrates.[29,65] Moreover, the functionalization of FETs with polymers bearing amino moieties has been recently reported for the anchoring of AchE in order to fabricate acetylcholinesterase sensors.[24] As a proof-of-concept for the use of PEDOT–PAH1 OECTs as biosensors, we employed the available amino moieties from PAH as anchoring sites for the electrostatic immobilization of the enzyme AchE. Moreover, we also took advantage of the improved pH response of the PAH-modified

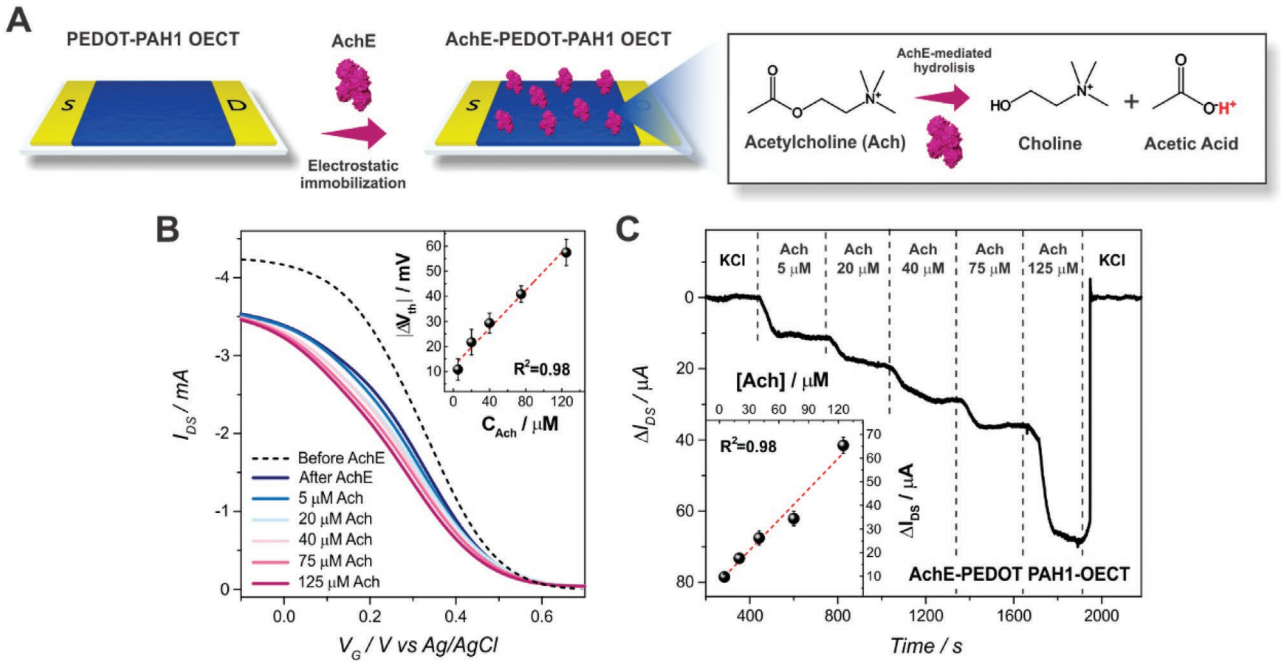

Figure 7. A) Scheme of the electrostatic immobilization strategy and the enzyme-catalyzed Ach hydrolysis. Transfer characteristics of an AchE-PEDOT–PAH1-OECT while varying Ach concentration (10 mM KCl, pH 7.4, V_D = –0.1 V). The inset shows the linear fitting of the response. B) The curve for the transistor before AchE immobilization is also shown. C) Ach flow sensing measurement for an AchE-PEDOT–PAH1 OECT while applying a gate voltage of 0.3 V and a V_D of –0.1 V (10 mM KCl, pH 7.4, flow rate = 300 μL min^{-1}).

transistors, as the signal transduction mechanism roots on the pH change caused by acetylcholine-catalyzed hydrolysis.

Following a procedure already reported,[24] the enzyme was electrostatically immobilized by employing an enzyme solution of higher pH than its PI, which conferred negative charges to it (**Figure** 7A). The electrostatic immobilization can avoid some of the disadvantages of covalent attachment, such as poor reproducibility and the risk of altering the functionality of the enzyme, as crucial groups can be engaged in the immobilization.[66,67] After AchE electrostatic anchoring (AchE-PEDOT PAH1 OECTs), the I_{DS} values of the devices diminishes (Figure 7B). This result has also been observed in previous works, and it has been attributed to the added capacitance of the top layer to the ionic circuit between the gate and the channel.[68]

As the transistors showed a low pH sensitivity at an ionic strength of 0.1 M KCl, we investigated the pH response of PEDOT–PAH1 OECTs when lowering the ionic strength down to 10 mM KCl, obtaining an enhancement of the pH sensitivity up to 14.5 mV/pH unit (Figure S14, Supporting Information).

Later, different concentrations of acetylcholine in pH 7.4 10 mM KCl solutions were prepared and used for the sensing experiments. First, the signal transduction mechanism of the biosensors was studied by analyzing the static response. The transfer characteristics of an AchE-PEDOT–PAH1 OECT for different Ach concentrations solutions are shown in Figure 7B. A clear shift of the threshold voltage to more negative potentials can be noticed in the presence of the enzyme substrate, which is consistent with a shift obtained upon decreasing the pH. This outcome reveals that AchE effectively catalyze the hydrolysis of acetylcholine, yielding choline and acetic acid and, thus, causing a decrease in the local pH (Figure 7A). Then, the pH variation modifies the charge density of the composite triggering a negative shift of the threshold voltage. Later, the devices showed a sensitivity of 4.0 ± 0.3 mV per Ach concentration decade.

Furthermore, the real-time flow response of AchE-PEDOT–PAH1 transistors to increasing Ach concentration solutions was studied, as it is shown in Figure 7C. In this setup, the gate voltage used corresponded to that of maximum transconductance of the transistors (V_G = 0.3 V). The lower V_{th} of the PEDOT–PAH1 OECTs as compared with PEDOT OECTs allows applying small gate voltages when sensing the analyte, which avoids enzyme disruption. As schemed in Figure 7A, the decrease on the local pH due to acetylcholine catalyzed hydrolysis shifts the threshold voltage of the transistors to more negative values, which causes a decrease in the absolute value of I_{DS} at a fixed gate potential. Then, the continuous flow response of the transistors shows that they can be used for the real-time sensing of Ach, showing a sensitivity of 4.4 ± 0.3 μA per Ach concentration decade. In this way, the high transconductances of the devices transduce the relatively small shift in V_{th} into an easily observable change in I_{DS}. Moreover, the transistors were able to detect Ach concentrations down to 5 μM, which allows for its further use as sensors in biological fluids, as, for example, the concentration of Ach in saliva has been reported to be around 8–9 μM.[69]

3. Conclusions

We have shown the successful fabrication of OECTs using PEDOT–PAH composites as channel material. The control of

the polyelectrolyte:PEDOT ratio allowed us to tune the electronic and ionic features while maintaining high values of transconductance, a crucial parameter for the development of high-performance bioelectronic devices. Together with the lower threshold voltages shown by PEDOT–PAH OECTs, this allowed the transistors to be operated at low gate voltages, which is an essential requirement for the successful integration of OECTs with biological systems. Furthermore, the PAH incorporation caused no additional barrier for ion migration during the dedoping/doping process but, on the contrary, it improved the transient response of the transistors, probably due to an enhanced ion transport throughout the channel material.

On the other hand, the incorporation of PAH in the channel material of the OECTs also enhanced the pH response of the transistors as a result of the inclusion of the pH-sensitive amino moieties. Particularly, PEDOT–PAH1 OECTs showed the highest pH sensitivity, probably due to an intimate connection between both polymers. Later, the polyamine also allowed for the functional electrostatic anchoring of an enzyme in order to construct biosensors. As a proof-of-concept, AchE was electrostatically immobilized by taking advantage of the NH_2 moieties, and the sensors were able to successfully monitor the neurotransmitter acetylcholine in the range 5–125 μM.

We believe that this work could pave the way for the development of devices capable to perform real-time monitoring of various biomarkers through the incorporation of different enzymes on the channel material. Finally, the integration of PEDOT–PAH OECTs in neuromorphic circuits together with their ability to sense acetylcholine could lead to the construction of devices allowing the simultaneous detection of the neurotransmitter together with the electronic recording of brain signals.

4. Experimental Section

Reagents and Materials: Acetylcholine chloride (≥99%), AchE from *Electrophorus electricus* (electric eel) (Type V-S, lyophilized powder, ≥1000 units/mg protein) (AchE), EtOH, KOH pellets, HCl, EDOT (97%), PAH ($M_w \approx 58$ kDa), and hexaaminеruthenium (II) chloride were obtained from Sigma Aldrich. Pyridine (99%) was purchased from Biopack and iron (III) *p*-toluenesulfonate (38–42% in 1-butanol) was obtained from Heraeus, while n-Butanol (99.4%), Acetone, and KCl were purchased from Anedra Technologies. Hexaaminеruthenium (III) chloride was purchased from Alfa Aesar. All solutions were prepared with Milli-Q Water. Interdigitated electrodes (IDEs) were obtained from Micrux (IDE1), while ITO plates (R_s = 5–15 Ω cm) were purchased from Delta.

Fabrication of the Organic Electrochemical Transistors: Commercial interdigitated gold electrodes (10/10 μm electrode/gap, ED-IDE1-Au, each IDE consisting of 90 pairs of interdigitated gold electrodes) (IDEs) were obtained from Micrux Technologies. Prior to modification, IDEs were cleaned with acetone and ethanol and dried. OECTs were prepared by in situ chemical polymerization of the channel material on the array area of the IDEs, following a modification of a previously reported protocol.[70] In order to fabricate PEDOT OECTs, an oxidant solution containing 715 μL of 40% Fe(III) tosylate butanol solution, 220 μL of butanol, and 16.5 μL of pyridine was prepared. Later, this solution was mixed with 12.5 μL of the EDOT monomer, homogenized in a vortex, and filtered (0.2 μm). Subsequently, the solution was spin coated onto the array area of the interdigitated electrodes at 1000 rpm for 1 min applying an acceleration of 500 rpm min^{-1}. Finally, the substrates were heated at 70 °C for 15 min, rinsed with Milli-Q water and dried with N_2. A similar procedure was followed for the preparation of the different PEDOT–PAH OECTs, while adding 200 μL of different PAH solutions (15 mg PAH in 200 μL Milli-Q water for PEDOT–PAH1, 40 mg for PEDOT–PAH2, and 75 mg for PEDOT–PAH3) to the polymerization solution. The effect of adding water to the polymerization solution in PEDOT transistors was evaluated and no change was observed in the obtained transistors.

Spectroelectrochemistry: ITO plates were modified with the different polymer blends by following the previously described procedure for the fabrication of the transistors and used as the working electrode. Spectroelectrochemistry measurements were performed with an Agilent 8453E diode array spectrophotometer in the spectral range between 300 and 1000 nm while applying different potentials to the working electrode. The setup comprised a 0.1 M KCl filled quartz cell in which the different modified ITO plates were perpendicularly immersed with respect to the light path. A Pt wire constituted the counter electrode while an Ag/AgCl electrode was used as reference electrode (see Section 2.2). The absorbances were normalized with respect to film thickness.

Electrochemical Measurements: The output, transfer, and transient characteristics of the transistors were obtained with a TEQ bipotentiostat system. The electrochemical cell used consisted in a batch add-on obtained from Micrux Technologies, using an Ag/AgCl (3 M KCl) as gate electrode.

CV and EIS measurements were performed in an Autolab potentiostat with both source and drain electrodes of the OECTs being connected as WE, while using an Ag/AgCl reference electrode and a Pt wire as CE. The electrolyte solution used was 0.1 M KCl. Potentiostatic EIS measurements were performed at 0 V in the frequency range from 1 to 10^5 Hz, while CV measurements were performed at 100 mV s^{-1}.

Acetylcholinesterase Electrostatic Immobilization: The AchE electrostatic immobilization was performed following a previously reported procedure.[24] As the isoelectric point of AchE was known to be 5.3, a 1 mg mL^{-1} solution of the enzyme in buffer (HEPES 0.1 mM, 10 mM KCl) was prepared and adjusted to pH 7.4 in order to induce the electrostatic anchoring. Afterward, the array area of the PEDOT PAH1-OECTs was immersed in the AchE solution for 30 min and rinsed with buffer solution. The modified transistors were stored at 4 °C.

Flow Measurement: An electrochemical flow-cell (Micrux) was used for the continuous flow measurements. The automatic sample collection was performed at a constant flow rate of 300 μL min^{-1} by a peristaltic pump (Ismatec) coupled to a switching valve (Rheodyne). Different pH solutions were prepared by dropwise addition of HCl or KOH to the buffer. For the sensing experiments, different concentration acetylcholine solutions were prepared in 10 mM KCl buffer and adjusted to pH 7.4.

Atomic Force Microscopy: AFM images were acquired in a dry air environment with a Keysight 9500 microscope. AC160TS (Al-coated, 300 kHz nominal frequency, 40 N m^{-1} nominal spring constant, Olympus) AFM probes were used.

Supporting Information

Supporting Information is available from the Wiley Online Library or from the author.

Acknowledgements

This work was supported by ANPCyT (PICT-2016-1680, PICT-2017-1523), CEST-Competence Center for Electrochemical Surface Technologies (CEST–UNLP Partner Lab for Bioelectronics), Universidad Nacional de La Plata (PID-X867). Dr. Luciano Sappia is greatly acknowledged for helping with the PEDOT–PAH composite preparation. G.E.F. acknowledges CONICET for a doctoral fellowship.

Conflict of Interest

The authors declare no conflict of interest.

Data Availability Statement

Research data are not shared.

Keywords

acetylcholine, bioelectronics, biosensing, organic electrochemical transistors, poly(3,4-ethylenedioxythiophene), polyamine

Received: January 19, 2021
Revised: April 7, 2021
Published online:

[1] D. Ohayon, S. Inal, *Adv. Mater.* **2020**, *32*, 2001439.
[2] E. Zeglio, A. L. Rutz, T. E. Winkler, G. G. Malliaras, A. Herland, *Adv. Mater.* **2019**, *31*, 1806712.
[3] S. Inal, J. Rivnay, A. O. Suiu, G. G. Malliaras, I. McCulloch, *Acc. Chem. Res.* **2018**, *51*, 1368.
[4] R. A. Picca, K. Manoli, E. Macchia, L. Sarcina, C. Di Franco, N. Cioffi, D. Blasi, R. Österbacka, F. Torricelli, G. Scamarcio, L. Torsi, *Adv. Funct. Mater.* **2020**, *30*, 1904513.
[5] M. Sensi, M. Berto, S. Gentile, M. Pinti, A. Conti, G. Pellacani, C. Salvarani, A. Cossarizza, C. A. Bortolotti, F. Biscarini, *Chem. Commun.* **2021**, *57*, 367.
[6] X. Guo, A. Facchetti, *Nat. Mater.* **2020**, *19*, 922.
[7] A. Savva, R. Hallani, C. Cendra, J. Surgailis, T. C. Hidalgo, S. Wustoni, R. Sheelamanthula, X. Chen, M. Kirkus, A. Giovannitti, A. Salleo, I. McCulloch, S. Inal, *Adv. Funct. Mater.* **2020**, *30*, 1907657.
[8] G. Sonmez, *Chem. Commun.* **2005**, *42*, 5251.
[9] G. E. Fenoy, B. Van der Schueren, J. Scotto, F. Boulmedais, M. R. Ceolín, S. Bégin-Colin, D. Bégin, W. A. Marmisollé, O. Azzaroni, *Electrochim. Acta* **2018**, *283*, 1178.
[10] J. F. Mike, J. L. Lutkenhaus, *J. Polym. Sci., Part B: Polym. Phys.* **2013**, *51*, 468.
[11] E. Smela, *Adv. Mater.* **2003**, *15*, 481.
[12] I. Uguz, C. M. Proctor, V. F. Curto, A. M. Pappa, M. J. Donahue, M. Ferro, R. M. Owens, D. Khodagholy, S. Inal, G. G. Malliaras, *Adv. Mater.* **2017**, *29*, 1701217.
[13] K. A. Ludwig, N. B. Langhals, M. D. Joseph, S. M. Richardson-Burns, J. L. Hendricks, D. R. Kipke, *J. Neural Eng.* **2011**, *8*, 014001.
[14] J. Rivnay, S. Inal, A. Salleo, R. M. Owens, M. Berggren, G. G. Malliaras, *Nat. Rev. Mater.* **2018**, *3*, 17086.
[15] E. Macchia, K. Manoli, C. Di Franco, R. A. Picca, R. Österbacka, G. Palazzo, F. Torricelli, G. Scamarcio, L. Torsi, *ACS Sens.* **2020**, *5*, 1822.
[16] D. Khodagholy, J. Rivnay, M. Sessolo, M. Gurfinkel, P. Leleux, L. H. Jimison, E. Stavrinidou, T. Herve, S. Sanaur, R. M. Owens, G. G. Malliaras, *Nat. Commun.* **2013**, *4*, 2133.
[17] S. Inal, G. G. Malliaras, J. Rivnay, *Nat. Commun.* **2017**, *8*, 1767.
[18] Y. Xuan, M. Sandberg, M. Berggren, X. Crispin, *Org. Electron.* **2012**, *13*, 632.
[19] S. T. Keene, T. P. A. van der Pol, D. Zakhidov, C. H. L. Weijtens, R. A. J. Janssen, A. Salleo, Y. van de Burgt, *Adv. Mater.* **2020**, *32*, 2000270.
[20] D. Minudri, D. Mantione, A. Dominguez-Alfaro, S. Moya, E. Maza, C. Bellacanzone, M. R. Antognazza, D. Mecerreyes, *Adv. Electron. Mater.* **2020**, *6*, 2000510.
[21] M. J. Donahue, A. Sanchez-Sanchez, S. Inal, J. Qu, R. M. Owens, D. Mecerreyes, G. G. Malliaras, D. C. Martin, *Mater. Sci. Eng., R* **2020**, *140*, 100546.
[22] Y. Xia, J. Ouyang, *ACS Appl. Mater. Interfaces* **2012**, *4*, 4131.
[23] N. Wang, A. Yang, Y. Fu, Y. Li, F. Yan, *Acc. Chem. Res.* **2019**, *52*, 277.
[24] G. E. Fenoy, W. A. Marmisollé, O. Azzaroni, W. Knoll, *Biosens. Bioelectron.* **2020**, *148*, 111796.
[25] S. Fabiano, S. Braun, X. Liu, E. Weverberghs, P. Gerbaux, M. Fahlman, M. Berggren, X. Crispin, *Adv. Mater.* **2014**, *26*, 6000.
[26] C. Cea, G. D. Spyropoulos, P. Jastrzebska-Perfect, J. J. Ferrero, J. N. Gelinas, D. Khodagholy, *Nat. Mater.* **2020**, *19*, 679.
[27] E. Zeglio, J. Eriksson, R. Gabrielsson, N. Solin, O. Inganäs, *Adv. Mater.* **2017**, *29*, 1605787.
[28] L. D. Sappia, E. Piccinini, C. von Binderling, W. Knoll, W. Marmisollé, O. Azzaroni, *Mater. Sci. Eng., C* **2020**, *109*, 110575.
[29] L. D. Sappia, E. Piccinini, W. Marmisollé, N. Santilli, E. Maza, S. Moya, F. Battaglini, R. E. Madrid, O. Azzaroni, *Adv. Mater. Interfaces* **2017**, *4*, 1700502.
[30] M. H. Chakrabarti, C. T. J. Low, N. P. Brandon, V. Yufit, M. A. Hashim, M. F. Irfan, J. Akhtar, E. Ruiz-Trejo, M. A. Hussain, *Electrochim. Acta* **2013**, *107*, 425.
[31] F. Buth, A. Donner, M. Sachsenhauser, M. Stutzmann, J. A. Garrido, *Adv. Mater.* **2012**, *24*, 4511.
[32] E. Stavrinidou, P. Leleux, H. Rajaona, D. Khodagholy, J. Rivnay, M. Lindau, S. Sanaur, G. G. Malliaras, *Adv. Mater.* **2013**, *25*, 4488.
[33] L. Kergoat, L. Herlogsson, B. Piro, M. C. Pham, G. Horowitz, X. Crispin, M. Berggren, *Proc. Natl. Acad. Sci. U. S. A.* **2012**, *109*, 8394.
[34] P. Schmode, D. Ohayon, P. M. Reichstein, A. Savva, S. Inal, M. Thelakkat, *Chem. Mater.* **2019**, *31*, 5286.
[35] J. Fan, S. S. Rezaie, M. Facchini-Rakovich, D. Gudi, C. Montemagno, M. Gupta, *Org. Electron.* **2019**, *66*, 148.
[36] E. Stavrinidou, O. Winther-Jensen, B. S. Shekibi, V. Armel, J. Rivnay, E. Ismailova, S. Sanaur, G. G. Malliaras, B. Winther-Jensen, *Phys. Chem. Chem. Phys.* **2014**, *16*, 2275.
[37] H. Talukdar, A. C. Bhowal, S. Kundu, *Phys. E* **2019**, *107*, 30.
[38] T. P. A. Van Der Pol, S. T. Keene, B. W. H. Saes, S. C. J. Meskers, A. Salleo, Y. Van De Burgt, R. A. J. Janssen, *J. Phys. Chem. C* **2019**, *123*, 24328.
[39] J. Wang, D. Ye, Q. Meng, C.-a. Di, D. Zhu, *Adv. Mater. Technol.* **2020**, *5*, 2000218.
[40] D. Khodagholy, J. Rivnay, M. Sessolo, M. Gurfinkel, P. Leleux, L. H. Jimison, E. Stavrinidou, T. Herve, S. Sanaur, R. M. Owens, G. G. Malliaras, *Nat. Commun.* **2013**, *4*, 2133.
[41] L. Groenendaal, G. Zotti, P. H. Aubert, S. M. Waybright, J. R. Reynolds, *Adv. Mater.* **2003**, *15*, 855.
[42] M. Berggren, G. G. Malliaras, *Science* **2019**, *364*, 233.
[43] G. C. Faria, D. T. Duong, A. Salleo, *Org. Electron.* **2017**, *45*, 215.
[44] D. A. Bernards, G. G. Malliaras, *Adv. Funct. Mater.* **2007**, *17*, 3538.
[45] E. Zeglio, M. Vagin, C. Musumeci, F. N. Ajjan, R. Gabrielsson, X. T. Trinh, N. T. Son, A. Maziz, N. Solin, O. Inganäs, *Chem. Mater.* **2015**, *27*, 6385.
[46] G. Horowitz, *Adv. Mater.* **1998**, *10*, 365.
[47] L. H. Jimison, A. Hama, X. Strakosas, V. Armel, D. Khodagholy, E. Ismailova, G. G. Malliaras, B. Winther-Jensen, R. M. Owens, *J. Mater. Chem.* **2012**, *22*, 19498.
[48] G. E. Fenoy, J. M. Giussi, C. von Bilderling, E. M. Maza, L. I. Pietrasanta, W. Knoll, W. A. Marmisollé, O. Azzaroni, *J. Colloid Interface Sci.* **2018**, *518*, 92.
[49] I. Rubinstein, *J. Electrochem. Soc.* **1987**, *134*, 3078.
[50] F. J. R. Nieto, R.-I. Tucceri, *J. Electroanal. Chem.* **1996**, *416*, 1.
[51] M. J. R. J. R. Presa, H. L. L. Bandey, R. I. I. Tucceri, M. I. I. Florit, D. Posadas, A. R. R. Hillman, *Electrochim. Acta* **1999**, *44*, 2073.
[52] J. Scotto, W. A. Marmisollé, D. Posadas, *J. Solid State Electrochem.* **2019**, *23*, 1947.
[53] V. A. Online, C. Musumeci, M. Vagin, E. Zeglio, L. Ouyang, R. Gabrielsson, O. Inganäs, *J. Mater. Chem. C* **2019**, *7*, 2987.
[54] M. Giordani, M. Sensi, M. Berto, M. Di Lauro, C. A. Bortolotti, H. L. Gomes, M. Zoli, F. Zerbetto, L. Fadiga, F. Biscarini, *Adv. Funct. Mater.* **2020**, *30*, 2002141.

[55] S. Demuru, B. P. Kunnel, D. Briand, *Adv. Mater. Technol.* **2020**, *5*, 2000328.
[56] E. Macchia, K. Manoli, B. Holzer, C. Di Franco, R. A. Picca, N. Cioffi, G. Scamarcio, G. Palazzo, L. Torsi, *Anal. Bioanal. Chem.* **2019**, *411*, 4899.
[57] Z. U. Khan, O. Bubnova, M. J. Jafari, R. Brooke, X. Liu, R. Gabrielsson, T. Ederth, D. R. Evans, J. W. Andreasen, M. Fahlman, X. Crispin, *J. Mater. Chem. C* **2015**, *3*, 10616.
[58] E. Mitraka, L. Kergoat, Z. U. Khan, S. Fabiano, O. Douhéret, P. Leclère, M. Nilsson, P. A. Ersman, G. Gustafsson, R. Lazzaroni, M. Berggren, X. Crispin, *J. Mater. Chem. C* **2015**, *3*, 7604.
[59] J. E. Yoo, K. S. Lee, A. Garcia, J. Tarver, E. D. Gomez, K. Baldwin, Y. Sun, H. Meng, T. Q. Nguyen, Y. L. Loo, *Proc. Natl. Acad. Sci. USA* **2010**, *107*, 5712.
[60] F. Mariani, I. Gualandi, M. Tessarolo, B. Fraboni, E. Scavetta, *ACS Appl. Mater. Interfaces* **2018**, *10*, 22474.
[61] G. Scheiblin, R. Coppard, R. M. Owens, P. Mailley, G. G. Malliaras, *Adv. Mater. Technol.* **2017**, *2*, 1600141.
[62] P. K. Johansson, D. Jullesson, A. Elfwing, S. I. Liin, C. Musumeci, E. Zeglio, F. Elinder, N. Solin, O. Inganäs, *Sci. Rep.* **2015**, *5*, 11242.
[63] E. Piccinini, C. Bliem, C. Reiner-Rozman, F. Battaglini, O. Azzaroni, W. Knoll, *Biosens. Bioelectron.* **2017**, *92*, 661.
[64] R. Pfattner, A. M. Foudeh, S. Chen, W. Niu, J. R. Matthews, M. He, Z. Bao, *Adv. Electron. Mater.* **2019**, *5*, 1800381.
[65] L. D. Sappia, E. Piccinini, C. von Binderling, W. Knoll, W. Marmisollé, O. Azzaroni, *Mater. Sci. Eng., C* **2020**, *109*, 110575.
[66] A. Vakurov, C. E. Simpson, C. L. Daly, T. D. Gibson, P. A. Millner, *Biosens. Bioelectron.* **2005**, *20*, 2324.
[67] R. A. Sheldon, S. van Pelt, *Chem. Soc. Rev.* **2013**, *42*, 6223.
[68] A. M. Pappa, S. Inal, K. Roy, Y. Zhang, C. Pitsalidis, A. Hama, J. Pas, G. G. Malliaras, R. M. Owens, *ACS Appl. Mater. Interfaces* **2017**, *9*, 10427.
[69] Z. T. Dame, F. Aziat, R. Mandal, R. Krishnamurthy, S. Bouatra, S. Borzouie, A. C. Guo, T. Sajed, L. Deng, H. Lin, P. Liu, E. Dong, D. S. Wishart, *Metabolomics* **2015**, *11*, 1864.
[70] L. D. Sappia, E. Piccinini, W. Marmisollé, N. Santilli, E. Maza, S. Moya, F. Battaglini, R. E. Madrid, O. Azzaroni, *Adv. Mater. Interfaces* **2017**, *4*, 1700502.

